JOINT CONFERENCE PROCEEDINGS
9th International Conference on Urban Earthquake Engineering/ 4th Asia Conference on Earthquake Engineering
March 6-8, 2012, Tokyo Institute of Technology, Tokyo, Japan

OBSERVATIONS FROM NEES/E-DEFENSE TESTS OF A FULL SCALE ISOLATED AND FIXED-BASE BUILDING

Keri L. Ryan[1)], Eiji Sato[2)], Tomohiro Sasaki[3)], Nhan D. Dao[4)], Taichiro Okazaki[5)]

1) Assistant Professor, Civil and Environmental Engineering, University of Nevada, Reno, USA
2) Senior Researcher, Hyogo Earthquake Engineering Research Center (E-Defense), National Research Institute for Earth Science and Disaster Prevention, Miki, Japan
3) Researcher, Hyogo Earthquake Engineering Research Center (E-Defense), National Research Institute for Earth Science and Disaster Prevention, Miki, Japan
4) PhD Candidate, Civil and Environmental Engineering, University of Nevada, Reno, USA
5) Associate Professor, Faculty and Graduate School of Engineering, Hokkaido University, Sapporo, Japan
keri.ryan@unr.edu, eiji@bosai.go.jp, tomo_s@bosai.go.jp, nhan.unr@gmail.com, tokazaki@eng.hokudai.ac.jp

Abstract: A 5-story steel moment frame building was tested at E-Defense in August of 2011 with three different support conditions: supported by triple friction pendulum isolation system, supported by lead rubber bearings in combination with cross linear bearings, and in the fixed-base condition. Nonstructural components and contents were installed on the 4th and 5th floors. The isolated buildings were subjected to strong excitations with the goal to approach the displacement limit of the base-isolation devices. The triple friction pendulum system was subjected to a variety of large ground motions, but did not reach its displacement limit as the friction was observed to be larger than during initial bearing characterization. The lead-rubber isolators were subjected simultaneously to large displacements and some tension. Nonstructural component damage and content disruption due to strong vertical excitation was observed in both isolation systems and in the fixed-base configuration.

1. INTRODUCTION

In August 2011, a monumental series of shake table tests were completed at the Hyogo Earthquake Engineering Research Center, otherwise known as E-Defense, of the National Research Institute of Earth Science and Disaster Prevention, through energized collaboration of U.S. and Japan researchers. In six total days of testing spanning a two week period, a 5-story steel moment frame building structure was shaken with two different seismic isolation systems and in the fixed base configuration. In total, the building structure was subjected to 41 sinusoidal and earthquake simulations including 13 distinct earthquake records, which is the greatest number and variety of simulations that has been performed in any test program at E-Defense to date. In particular, the building in the base-isolated configuration was subjected to very large earthquakes, several times pushing the E-Defense shaking table to its limit.

The overarching objective of the test program was to provide a full scale demonstration of the effectiveness of base isolation to protect not only the building structure, but also the nonstructural components and contents in very rare earthquakes. To this end, the building structure was augmented with a variety of nonstructural components and contents. On the 4th and 5th floors of the structure, an integrated system of interior walls, suspended ceilings and piping was assembled using U.S. construction techniques. The architectural layout included enclosed areas on each floor, which allowed for the enactment and portrayal of a hospital room and an office room including a variety of furniture and other loose items. In addition, a full story pre-cast concrete cladding column cover assembly was fabricated on the 4th floor to evaluate the effectiveness of current slotted steel connection design to allow inter-story drift. The performance of these nonstructural systems and contents is not the focus of this paper.

The two isolation systems designed and tested as part of this program were: 1) triple friction pendulum bearings (TPBs), and 2) a combined system of lead-rubber bearings (LRBs) and cross linear bearings (CLBs). The TPB isolation system was designed to provide continued functionality in a maximum considered earthquake ground motion, while the LRB/CLB system was selected with consideration to the performance objectives of nuclear power plants. Another objective of the program was to demonstrate the ability to extend seismic resiliency to challenging configurations, as the isolation systems were strategically selected to accommodate a relatively lightweight (relative to a typical isolation system design) and asymmetric superstructure. The earthquake excitations were carefully selected to excite the isolation systems to their displacement limits, which was

controlled by the physical limit of travel in the TPB system and stability considerations in the LRB/CLB system. A final objective was to determine the influence of vertical excitation on the performance of seismically-isolated buildings. In all three support configurations, the building was subjected to a variety of XY (horizontal only) and 3D excitations, including considerably large vertical accelerations. This paper highlights preliminary results and observations pertaining to the response of the isolation systems and the building structure.

2. BUILDING FRAME SPECIMEN

The specimen used throughout the test program was a 5-story steel moment frame building that was used as part of a previous test program (Figure 1). The specimen was constructed in September 2008 and tested in March 2009 with several different types of inter-story dampers to provide enhanced performance (Kasai et al. 2010). All dampers were removed from the building for the present seismic isolation experiments. This building specimen is approximately 16 meters tall, and asymmetric in plan with dimension of 10 meters by 12 meters (2 bays by 2 bays).

The specimen was designed and detailed according to Japanese code and design practice. The beams and girders are built-up or rolled wide flange sections, and the columns are cold-formed HSS sections. All girder-to-column and column base connections are fully restrained moment connections. Each girder was constructed in 3 pieces, and spliced by high-strength bolts at the approximate inflection points determined by gravity loading. The flanges of the girders are widened near the connections to the column to limit yielding near the critical welds. Floor slabs are composite slabs formed from 75-mm high corrugated steel decks covered by 80-mm normal concrete. The roof slab is a 150-mm normal concrete slab with a flat steel deck; the roof was designed to carry additional loading representative of equipment. Additional details of the building design and configuration are provided in Kasai et al. (2010). For the 2011 experiments, additional mass in the form of steel plates was placed on the roof in an irregular configuration to enhance the asymmetry of the building specimen (Figure 2). At 535 kN, this supplementary weight far exceeds the concentrated weight introduced by a typical roof mounted piece of equipment, such as a chiller (about 80 kN).

The design weight of the building, including known adjustments for configuration changes relative to earlier tests, is about 5,300 kN (1,200 kips), which is similar to the measured weight of the building specimen from load cells (described later). Table 1 summarizes the design weight and the estimated offset of the center of mass relative to the geometric center of the building in the x and y-directions. The dynamic properties of the building measured and reported from previous tests are: natural period = 0.68 sec, damping ratio = 2%. The modeling and analysis of the building specimen for 2011 experiments will be reported in future papers; preliminary results suggest the specimen in

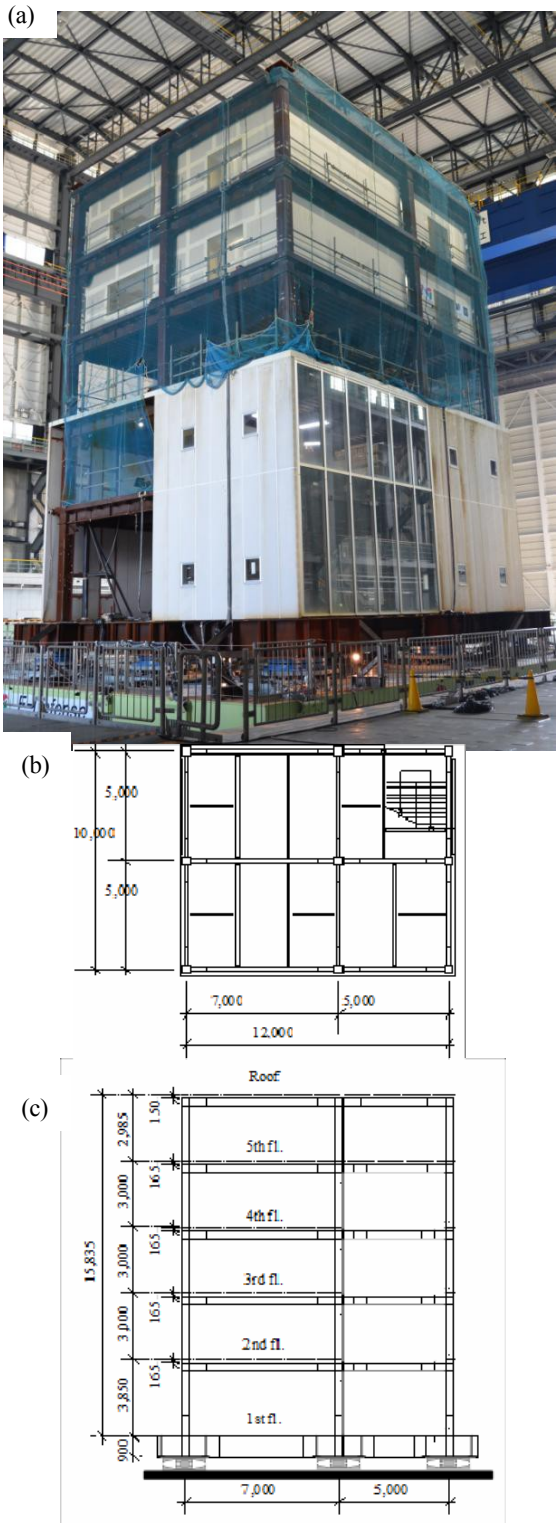

Figure 1 5-story steel moment frame specimen w/ triple pendulum isolators: (a) on shaking table, (b) plan view, and (c) elevation view.

the fixed-base configuration may have responded with slightly longer period and greater damping ratio than in previous tests. Such behavior may have been the result of

further accumulation of damage in concrete slabs from all prior tests.

3. DESIGN OF THE ISOLATION SYSTEMS

Two considerations influenced the design of both isolation systems. First, the isolation systems were to accommodate a relatively lightweight structure that weighed only about W = 5,300 kN (1,200 kips), leading to an average axial load of only about 600 kN (133 kips) per bearing when bearings are placed under all columns. Second, as previously noted, the system is asymmetric for shaking in the x-direction especially with the roof mass.

The first isolation system incorporated 9 identical TPBs, one beneath each column, which were manufactured by Earthquake Protection Systems (Figure 3). The properties of these isolators were chosen to accommodate the largest near fault ground motions that could be replicated by the E-Defense table. The bearings are 1.4 m (55 in) in diameter (Figure 3(b)), and provide a displacement capacity 1.13 m (44 in) with anticipated base shear coefficient V/W = 0.275, where V = isolator shear force and W = weight (Figure 4(a)). Under typical loading, sliding alternates on the inner pendulum surfaces (period T = 1.84 s) and outer pendulum surfaces (period T = 5.57 s), with sliding on the outer pendulums first occurring when the base shear coefficient V/W reaches about 0.08. Prior to reaching the displacement

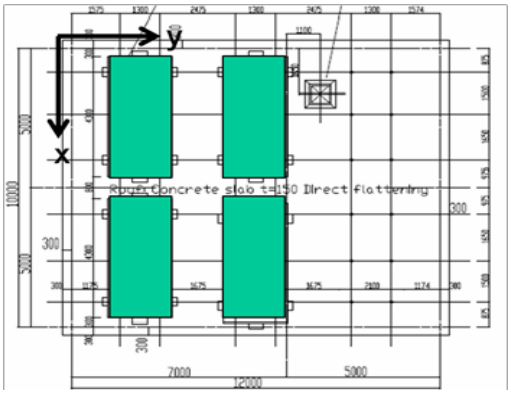

Figure 2 Supplementary steel plate mass (in green) superimposed on roof plan

Table 1 Seismic Weight and Offsets

Level	Design Weight (kN)	(m, %)	(m, %)
Roof	1170(*)	0.00, 0%	-1.15, 9.6%
5	808	0.18, 1.8%	-0.39, 3.3%
4	834	0.19, 1.9%	-0.23, 1.9%
3	829	0.23, 2.3%	-0.19, 1.6%
2	828	0.22, 2.2%	-0.26, 2.2%
Base	842	-0.05, 0.5%	0.45, 3.8%

(*) Includes 535 kN of steel plate weight

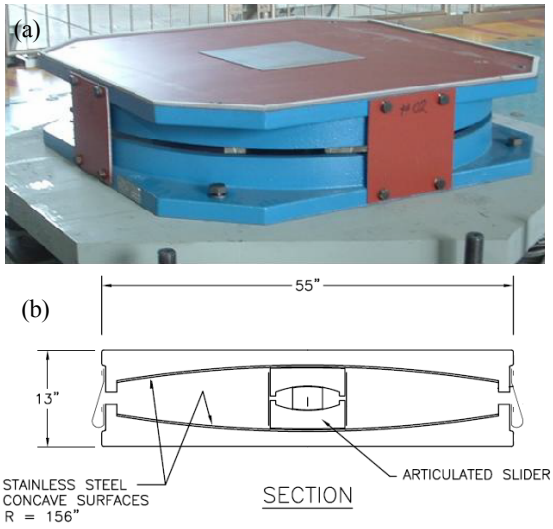

Figure 3 (a) Photograph and (b) section view (indicating sliding surfaces) of TPBs used in the test program

limit, the bearings will stiffen at 1.1 m (43.3 in) (base shear coefficient V/W = 0.214) as the limit of travel on the outer pendulum surfaces is reached and sliding transitions back to the inner pendulum (Figure 4(a)). This stiffening behavior is intended to slow the sliding and minimize the intensity of the impact that might occur at the displacement limit. The light structural weight and moderate structural asymmetry were of minor influence for the triple pendulum bearings, since the shear resistance generated by a friction device is proportional to the weight carried. As such, the isolation period is independent of the weight carried, and the lateral resistance of the isolation system is naturally balanced with the distribution of the mass above.

The second isolation system, featuring 4 LRBs manufactured by Dynamic Isolation Systems as the primary isolation devices, was designed to protect a nuclear power plant in beyond design basis shaking. The design basis shaking was evaluated for a representative soil site in eastern U.S., wherein the design spectrum was derived by converting the uniform hazard spectrum for an annual probability of exceedance of 10^{-4} to a uniform risk spectrum (Huang et al. 2009). In order to accommodate the light mass and overturning moments, the LRBs (Figure 5(a)) were supplemented with 5 CLBs (Figure 5(c)) manufactured by THK according to design specified by Aseismic Devices Company. The LRBs were each 700 mm (27.5 in) in diameter with a 102 mm (4 in) lead core and a shape factor S = 29. The ratio of lead core to bearing diameter is slightly below the range of 1/6 to 1/3, which has been considered by some to be ideal (Buckle et al. 2006). Assuming a constant axial force of 1325 kN (300 kip) per bearing based on the tributary gravity load, these LRBs provide a yield strength coefficient V/W = 0.055 and a post-yield period of T = 2.86 sec (Figure 4(b)). The CLBs are essentially low friction sliders that share the vertical load with the LRBs without increasing the stiffness or base shear of the isolation system.

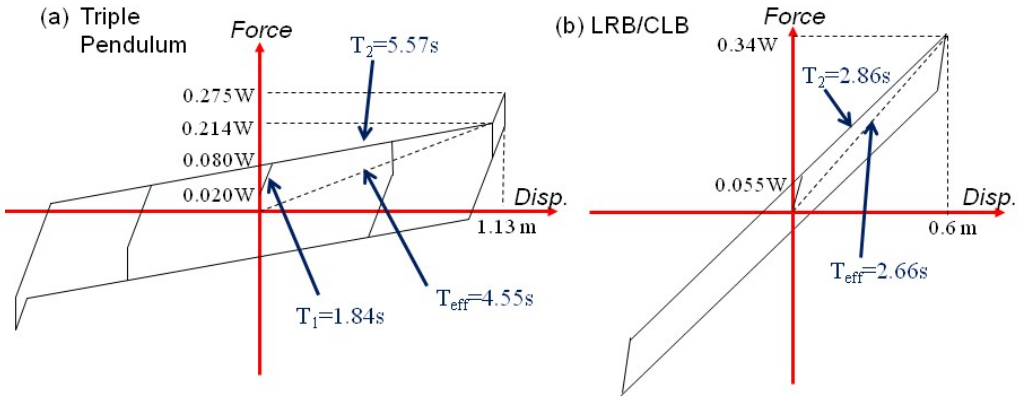

Figure 4 Force-displacement of the composite isolation system for (a) TPB system, and (b) LRB/CLB system

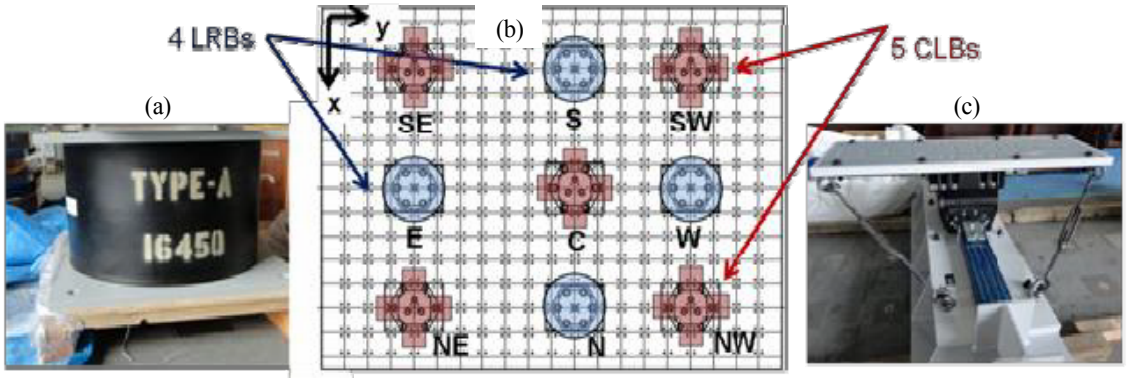

Figure 5 (a) Photograph of LRB, (b) plan layout of LRB/CLB, and (c) photo of CLB. Bearing position labels and direction of shaking are clarified.

The friction coefficient of the CLBs is given by

$$\mu = (1.2 + 3.6P_v / P_0) / 1000 \qquad (1)$$

where P_v is the axial force and P_0 is a reference force of 2451 kN. Furthermore, the CLBs enhance the global stability of the system by allowing the axial force to naturally redistribute between the LRBs and the CLBs, while also providing tension resistance. This combination of devices provided an anticipated base shear coefficient V/W = 0.34 at a displacement limit of 0.6 m (24 in), wherein the limit was determined by stability considerations in the LRBs rather than the limiting shear strain.

The LRB-CLB system placed LRBs at the edge locations and CLBs at the center and corner locations (Figure 5(b)). This arrangement offset the stiffness center of the isolated layer 0.5 m to the y-direction from the geometric center, which is opposite of the mass offset (Table 1).

4. OVERVIEW OF TEST PROGRAM

The building shaking schedule was as follows: 1) three days shaking for the TPB isolation system, 2) two days shaking for the LRB/CLB system, and 3) one day shaking for the fixed-base configuration, with about 7 strong excitations per day. Table 2 lists the primary shakings performed for each system, including scale factors and target peak accelerations. In many simulations the output peak table accelerations was larger than the target, but the output spectra showed good agreement with the target over the relevant period range.

The schedule for the TPB system was selected with the objective of subjecting the system to a wide variety of strong ground motions with different characteristics, such as intense high frequency content (e.g. JMA Kobe), near-fault (e.g. Sylmar and Takatori), very long period (e.g. Chi-chi TCU065 and Tabas), and long duration subduction (e.g. Tohoku-Iwanuma). Some excitations were repeated at different scale factors to incrementally and safely approach the displacement limits of the bearings. The schedule for the LRB/CLB system was selected with the objective of approaching the displacement limit of the system using synthetic motions representative of nuclear sites (Vogtle on the east coast and Diablo Canyon on the west coast) (Huang et al. 2009). The schedule for the fixed-base building was selected with the objective of strategically comparing the response of the isolated and fixed-base buildings; wherein the fixed-base records were necessarily scaled down to limit the structure response to the safe (linear) range.

Table 2 Schedule of Realized Excitations on Test Days

System	Test Date	Ground motion	Scale Factor	Peak $A_{,,Y}$ (g)	Peak $A_{,}$ (g)
Triple Pendulum Bearings (TPB)	Day 1 8117/11	Sine Wave (X)	65%	0,11	0
		Sine Wave (X)	100%	0,17	0
		1987 Superstition Hills - Westmorland (3D)	80%	0,17	0,20
		1940 Imperial Valley - El Centro (3D)	UO%	OA1	0,27
		1994 N01thridge–Rinaldi Rec, Sta, (3D)	88%	0,72	0,73
		1994 NOI1 hridge–Sylmar (3D)	100%	0,84	0,53
		1978 Tabas–Tabas Sta, (3D)	50%	*OA1*	0,34
	Day 2 8/18/11	1989 Loma Prieta –Los Gatos (3D)	70%	0,67	0,62
		1999 Chichi –TCU065 (XY)	50%	*OAO*	0
		1999 Chichi –TCU065 (XY)	70%	0,57	0
		2011 Tohoku-Iwanuma (XY)	100%	*OA3*	0
		Sannomam (XY)	100%	0,19	0
		1995 Kobe–Takatori (3D)	100%	0,74	0,28
		1995 Kobe–JI\!IA Kobe (3D)	100%	0,82	0,34
	Day *3* 8/19/11	1994 N01thridge–Rinaldi Ree, Sta, (XY)	88%	0,72	0
		1999 Chichi –TCU065 (XY)	80%	0,65	0
		1978 Tabas–Tabas Sta, (3D)	80%	0,68	0,55
		1978 Tabas–Tabas Sta, (XY)	90%	0,76	0
		1978 Tabas–Tabas Sta, (XY)	100%	0,85	0
		1985 Mexico City –SCT (XY)	100%	0,17	0
		1995 Kobe–Takatori (3D)	115%xy 100%z	0,85	0,28
Lead Rubber Bearings and Cross Linear Bearings (LRB/ CLB)	Day 4 8/25/11	1987 Superstition Hills - vVestmorland (3D)	80%	0,17	0,20
		Sine Wave (Y)	100%	0,29	0
		Vogtle #U (3D)	75%	*0,33*	0,22
		Vogtle #U (3D)	100%	*OA4*	0,29
		Vogtle #U (3D)	125%	0,56	0,36
		Vogtle #13 (3D)	150%	0,67	*OA4*
		Vogtle #U (3D)	175%	0,78	0,51
		Diablo Canyon #28 (3D)	80%	0,79	0,70
	Day 5 8/26/11	Diablo Canyon #28 (XY)	95%	0,93	0,83
		1940 Imperial Valley - El Centro (3D)	UO%	0A1	0,27
		2011 Tohoku-Iwanuma (XY)	100%	*OA3*	0
		1994 N01thridge–Rinaldi Ree, Sta, (XY)	88%	0,72	0
		1994 Northridge–Rinaldi Rec, Sta, (3D)	88%	0,72	0,73
		Vogtle #13 (3D)	75%	0,33	0,22
		Sine Wave (Y)	100%	0,29	0
Fixed Base	Day 6 8/31l11	1987 Superstition Hills - Westmorland (3D)	80%	0,17	0,20
		1994 Northridge–Rinaldi Rec, Sta, (XY)	35%	0,28	0
		1994 N01thridge–Rinaldi Rec, Sta, (3D)	35%	0,28	0,29
		1994 NOI1 hridge–Rinaldi Rec, Sta, (3D)	35%xy 88%z	0,28	0,73
		2011 Tohoku-Iwanuma (XY)	70%	0,30	0

5. INSTRUMENTATION

An extensive instrumentation plan was developed and executed that included more than 650 channels, Isolator lateral deformations were recorded using DTP-D-5KS wire potentiometers with a stroke limit of ±2,5 m, An assembly of load cells was used to measure lateral and vertical forces of each bearing in a configuration that has been described previously (Dao et aL 2011), In the LRB/CLB system, forces were measured in the LRBs only, Bidirectional story drifts were recorded at two locations (SE and NW quadrant) on every floor by laser displacement transducers attached to a rigid vertical truss, Floor accelerations were recorded at each level by 3D accelerometers attached at theSE, NE and NW columns,

6. EARLY OBSERVATIONS FROM THE TESTS

6.1 Response of TPB at Large Displacement Demands

The largest displacement in the TPBs was observed in 100% Tabas XY on Day 3 (Table 2). The realized peak vector displacement demand in the bearings was about 700 mm (27.6 in) (Figure 6(c, f)), which was well short of the expected displacement near 1 m (39.4 in) for this motion. Analysis using a simplified single degree-of-freedom (SDOF) bidirectionally coupled model with the characterized properties of the bearings (Figure 5(a)) predicts a displacement demand of 1.05 m (41.3 in). Further analysis suggests that during the E-Defense tests, the TPBs responded with effective friction greater than observed during characterization tests. Full speed characterization tests conducted by EPS (data not shown here) produced hysteretic loops that correspond closely to the idealized behavior in Figure 5(a). However, characterization of the unidirectional sine wave tests suggests that the realized friction of the outer sliding surfaces in the shake table test was larger than the value determined from initial

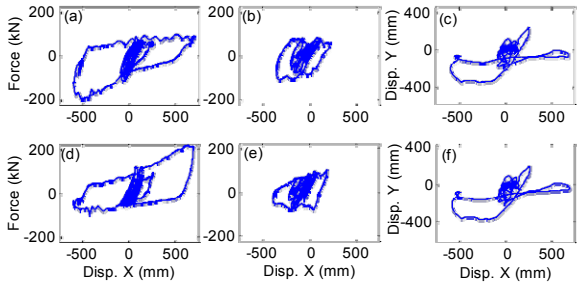

Figure 6 Recorded data for TPB in 100% Tabas XY; force vs. disp. in x, y and displacement trace for (a-c) SE bearing, and (d-f) NE bearing

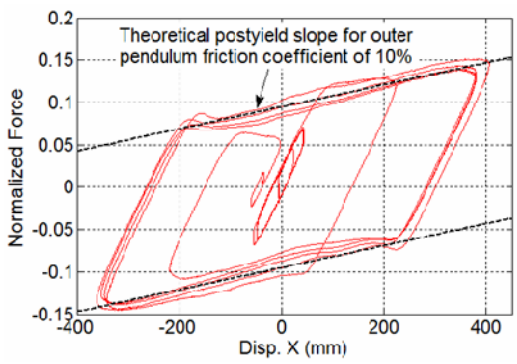

Figure 7 Normalized force vs. displacement for bearing C in 100% Sine Wave X.

manufacturer supplied full speed characterization tests (about 8%). For instance, Figure 7 shows the normalized force vs. displacement for the center bearing, where dotted lines that match the theoretical stiffness of the outer pendulum have been super-imposed over the test data. These lines correspond to a friction coefficient of 10%.

The reason for the increase in friction in the TPB devices during testing at E-Defense relative to characterization is currently under investigation. The following factors are acknowledged: (1) The support plates separating the bearings from the load cells may not have been sufficiently rigid to stabilize and keep the bearings flat and level. (2) The grout layer between the bearings and the structure was incomplete as constructed and may have generated further incongruency in the sliding surface. On a positive note, the TPB isolation system accommodated all selected ground motions safely without reaching its displacement limit.

The unnormalized hysteresis loops for individual bearings exhibit fluctuation that can be attributed to variations in axial load. A large displacement pulse and associated overturning in the x-direction caused the axial force in the SE bearing to increase/decrease (and the hysteresis loop to expand/shrink) when the displacement is negative/positive, respectively (Figure 6(a-c)). The opposite effect is observed in the NE bearing (Figure 6(d-f)). This type of behavior in friction pendulum bearings is known and well documented (e.g. Morgan and Mahin 2011). In general, the lateral stiffness and resistance of a bearing is a function of axial load, which causes the local variations in force (e.g. over the largest displacement cycle in Figure 6(a)). The effect is moderate in the 100% Tabas XY excitation, but becomes more pronounced when vertical excitation is present.

6.2 Response of LRB/CLB at Large Displacement Demands

The largest displacement in the LRB/CLB system was observed in 95% Diablo Cyn XY on Day 5 (Table 2). The realized peak vector displacement was 547 mm (21.5 in) in bearing E (Figure 8(c)) and in the opposite side bearing W (Figure 8(f)) was 412 mm (16.2 in). The measured displacement in the 95% motion closely matched the prediction to reach 550 mm (21.7 in) in the 100% motion. In general, the measured response was close to the pre-test analysis results for the LRB-CLB system.

The LRB-E and W hysteresis loops (Figures 8(a-b), 8(d-e)) are relatively smooth, with some notable pinching near the center (typical for a bearing with a small lead core) and minor variances likely due to bidirectional interaction. To examine the influence of axial load variations on the bearing hysteresis loops, the history of bearing displacement and axial force was plotted for each LRB (Figures 9(a-d)). The axial force data (Figure 9(d)) suggests that instances of greatest axial *unloading* generally correspond to instances of peak deformation (whether positive or negative) in all bearings (Figure 9(c)). In fact, LRB-E exhibited tension for several deformation peaks in a row. A summation of the axial force over all LRBs (Figure 9(e)) conveys the net axial unloading of the LRBs, which indicates that a net transfer of axial force from the LRBs to the CLBs at large deformation demands must have taken place. This force transfer occurs because the LRBs naturally shorten at large deformations, but were constrained from shortening by the base diaphragm and the high vertical stiffness of the CLBs. Since the compressive force on the LRBs never became large, the

LRBs and CLBs worked well together to isolator instability in this system. Evidently, for the specimen tested in this program, the axial unloading of LRBs at large displacements completely offset any increases in compressive force of the LRBs due to overturning. For instance, bearing LRB E appears to accumulate tension at every local peak (positive and negative deformation), which would correspond to

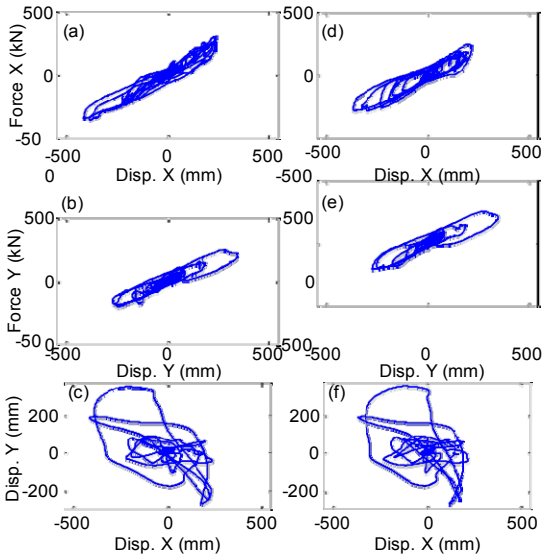

Figure 8 Recorded data for LRB/CLB 95% in Diablo Cyn 28 XY; hysteresis in x, y and displacement trace for (a-c) E bearing, and (d-f) W bearing

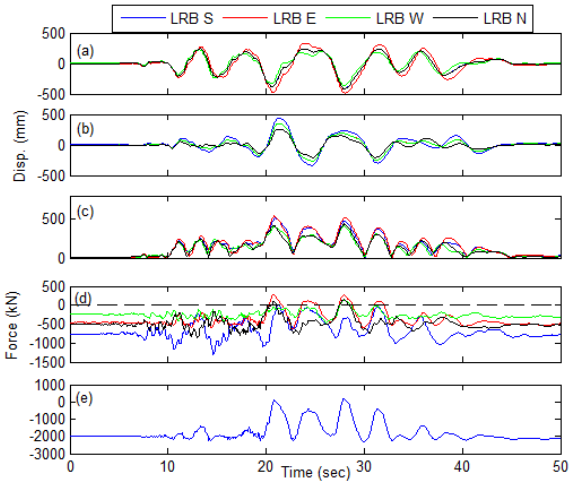

Figure 9 Recorded data for LRB in 95% DC 28; (a-c) x, y, and vector sum disps, (d) axial force in individual LRBs, and (e) sum axial force

instances of both positive and negative overturning. This phenomenon merits further investigation.

In this 95% Diablo Cyn simulation, the recorded tensile force in bearing LRB E was about 300 kN (67 kips) (Figure 9(d)), while over the entire series of simulations, a maximum tensile force of about 500 kN (112 kips) was observed. The manufacturer indicated that LRBs may be designed for an allowable stress up to 1.5G in tension (G = shear modulus), corresponding to about 240 kN (54 kips) in these LRBs, but that tensile capacities much larger than this have been observed in testing. The cyclic response of the LRBs did not appear to be affected by enduring the repeated tension demands generated by the test program.

6.3 Influence of Vertical Excitation on the Response of the Isolation Systems

One of the most noteworthy observations of the test was the influence of vertical excitation on the response of the isolated buildings. Damage to the nonstructural components on the 4th and 5th floor and notable content disruption was observed in all system configurations (TPB, LRB-CLB, and fixed base) during motions that included large components of vertical excitation. While base isolation is well known to provide no protection against vertical excitation, the level of disruption that could be attributed to vertical excitation was unexpected.

The Northridge Rinaldi Rec. Sta. (RRS) excitation with 88% scale factor caused the greatest level of disruption in all systems, and the peak table acceleration in each direction was observed to be on the order of 1.5-2 times the target, accompanied by a comparable increase in the response spectrum of the motion over the period range of 0-0.5 seconds. The motion was replicated with similar intensity and frequency content for all systems and on the empty table. While the motion produced by the table represents shaking considerably larger than 88% RRS for short period response, it was not thought to be unrealistic.

Corresponding to the observed damage and disruption, both horizontal floor accelerations and story drifts in the isolated building appear to be significantly amplified when the vertical component of excitation is present. Figure 10 compares recorded floor accelerations (5th and roof level) and story drifts (1st and 2nd level) for the TPB system subjected to 88% RRS XY and 3D excitations. Figure 11 shows the same set of results for the LRB-CLB system. In the TPB system, the upper story floor accelerations are increased from about 0.3g for XY excitation to about 0.9g for 3D excitation (Figure 10(b), 10(d)). This latter value is comparable to the PGA, and would thus suggest a diminished benefit of seismic isolation. The increase seems to be attributed to high frequency oscillation that is absent under XY excitation, and suggests a lateral/vertical coupling phenomenon. The story drift histories also exhibit the high frequency oscillation but the influence on peak drifts is moderate. The increase in accelerations and drifts are also observed in the LRB/CLB system (Figure 11), but does not appear to be as strong as in the TPB system.

One explanation for the difference in response accelerations between TPB and LRB-CLB bearing response is that several of the TPB system isolators were subjected to multiple uplift excursions and subsequent pounding when the device(s) made renewed contact with the table. The LRB-CLB system did not permit uplift but instead engaged the tensile resistance of both devices. No appreciable difference in damage or disruption was noted for the TPB system compared to the LRB/CLB system. Some of the

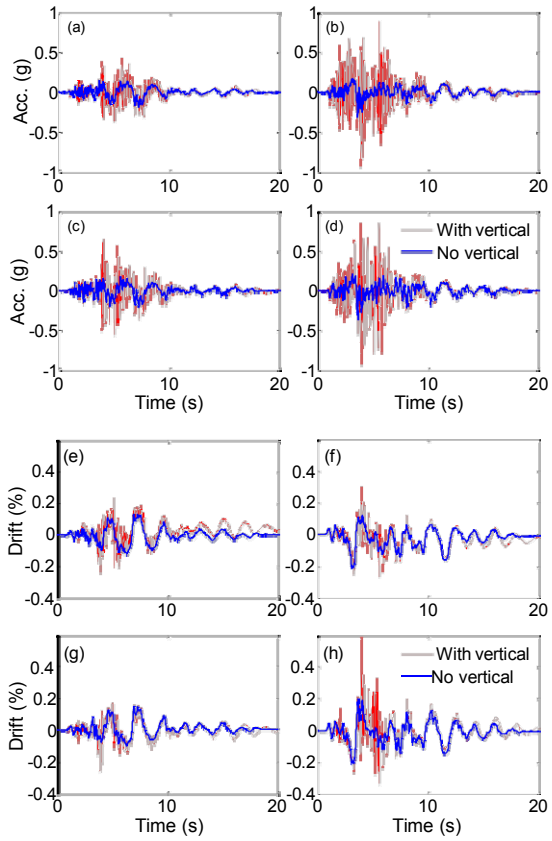

Figure 10 Recorded data for TPB subjected to RRS XY and 3D: accelerations in (a, b) 5th level x, y, (c, d) roof level x, y; story drift in (e, f) 1st story x, y, and (g, h) 2nd story x, y.

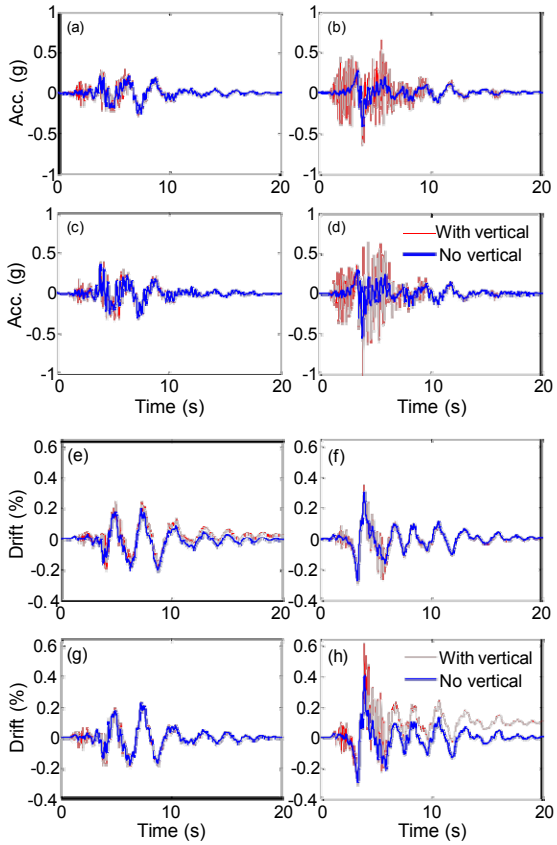

Figure 11 Recorded data for LRB/CLB subjected to RRS XY and 3D: accelerations in (a, b) 5th level x, y, (c, d) roof level x, y; story drift in (e, f) 1st story x, y, and (g, h) 2nd story x, y.

same characteristic high frequency response was also observed in the acceleration histories of the fixed-base system (not shown here), but did not appreciably influence the peak accelerations.

Although not shown here, significant amplifications in vertical acceleration (relative to the ground) also occurred. The lateral-vertical coupling and amplification of horizontal and vertical accelerations was a real phenomenon in this structure, and will be explained in future publications. However, it would be premature to draw general conclusions about the influence of vertical excitation on base-isolated structures.

3. CONCLUDING REMARKS

The test data from the E-Defense tests has the potential to transform our views on how to provide continued functionality after strong earthquakes. The isolation systems eliminated structural damage in motions that would likely have induced severe damage or possibly collapse of the fixed-base structure. At the same time, many interesting phenomena were revealed with regard to behavior of the full scale isolation devices, interaction of the response due to horizontal and vertical excitation, and the performance of nonstructural components and contents in both the seismic isolation and fixed base configurations. The data from this test is a rich resource to be unveiled in the months and years to come.

Acknowledgements:

This work was partially supported by the National Science Foundation through Grants No. CMMI-1113275 and CMMI-0721399, and U.S. Nuclear Regulatory Commission through Contract NRC-HQ-11-C-04-0067. Product donations were provided by Earthquake Protection Systems, Dynamic Isolation Systems, THK and Aseismic Devices Company. The authors are grateful for this support. The findings and opinions expressed in this paper are those of the authors, and do not necessarily reflect the views of the National Science Foundation, or the U.S. Nuclear Regulatory Commission.

References:

Buckle, I., Constantinou, M., Dicleli, M., and Ghasemi, H. (2006). *Seismic Isolation of Highway Bridges, Special Report MCEER-06-SP07.*

Dao, N., et. al. (2011). "Experimental evaluation of an innovative isolation system for a lightweight steel moment frame building at E-Defense", *Proc., ASCE Structures Congress*, Las Vegas, NV, April.

Huang, N.Y., Whittaker, A.S., Kennedy, R.P., and Mayes, R.L. (2009). "Assessment of Base-Isolated Nuclear Structures for Design and Beyond-Design Basis Earthquake Shaking", *Tech.*

Report MCEER-09-0008, University at Buffalo.
Kasai, K., et. al. (2010). "Full scale shake table tests of 5-story steel building with various dampers," *Proc., 7th Intern. Conf. on Urban Earthquake Engin. & 5th Intern. Conf. on Earthquake Engin.* Tokyo Inst. Tech., Tokyo, Japan.
Morgan, T. A. and Mahin, S. A. (2011). "The Use of Base Isolation Systems to Achieve Complex Seismic Performance Objectives", *PEER Report 2011/06*, Pacific Earthquake Engineering Center, University of California, Berkeley.